Developmental Biology 430 (2017) 142–155

Contents lists available at ScienceDirect

Developmental Biology

journal homepage: www.elsevier.com/locate/developmentalbiology

Original research article

Wnt signaling positively regulates endothelial cell fate specification in the Fli1a-positive progenitor population via Lef1

Kathleen Hübner[a,b,1], Kathrin S. Grassme[a,1], Jyoti Rao[c,d], Nina K. Wenke[a], Cordula L. Zimmer[e], Laura Korte[a], Katja Müller[c], Saulius Sumanas[f], Boris Greber[c,d], Wiebke Herzog[a,b,c,*]

[a] University of Muenster, Muenster, Germany
[b] Cells-in-Motion Cluster of Excellence (EXC 1003 – CiM), University of Muenster, Germany
[c] Max Planck Institute for Molecular Biomedicine, Muenster, Germany
[d] Chemical Genomics Centre of the Max Planck Society, Dortmund, Germany
[e] Ulm University, Ulm, Germany
[f] Division of Developmental Biology, Cincinnati Children's Hospital Medical Center, Cincinnati, OH, USA

ARTICLE INFO

Keywords:
Primitive hematopoiesis
Vasculogenesis
Wnt reporter
Mesoderm
Zebrafish

ABSTRACT

During vertebrate embryogenesis, vascular endothelial cells (ECs) and primitive erythrocytes become specified within close proximity in the posterior lateral plate mesoderm (LPM) from a common progenitor. However, the signaling cascades regulating the specification into either lineage remain largely elusive. Here, we analyze the contribution of β-catenin dependent Wnt signaling to EC and erythrocyte specification during zebrafish embryogenesis.

We generated novel β-catenin dependent Wnt signaling reporters which, by using destabilized fluorophores (Venus-Pest, dGFP), specifically allow us to detect Wnt signaling responses in narrow time windows as well as in spatially restricted domains, defined by Cre recombinase expression (*Tg(axin2$_{BAC}$:Venus-Pest)^{mu288}*; *Tg(14TCF:loxP-STOP-loxP-dGFP)^{mu202}*). We therefore can detect β-catenin dependent Wnt signaling activity in a subset of the Fli1a-positive progenitor population. Additionally, we show that mesodermal Wnt3a-mediated signaling via the transcription factor Lef1 positively regulates EC specification (defined by *kdrl* expression) at the expense of primitive erythrocyte specification (defined by *gata1* expression) in zebrafish embryos.

Using mesoderm derived from human embryonic stem cells, we identified the same principle of Wnt signaling dependent EC specification in conjunction with auto-upregulation of LEF1.

Our data indicate a novel role of β-catenin dependent Wnt signaling in regulating EC specification during vasculogenesis.

1. Introduction

To supply the body with oxygen and nutrients, vertebrates developed the cardiovascular system consisting of the heart, the vasculature, and the blood cells. All these components are mesoderm-derived structures, and their development is tightly linked to each other. Especially vascular endothelial cells (ECs) and primitive hematopoietic lineages arise in close proximity to each other during the first stages of embryonic development (Palis and Yoder, 2001; Risau and Flamme, 1995). The existence of a progenitor cell population with the capability to give rise to either of the lineages has been shown *in vitro* and *in vivo* (Choi et al., 1998; Haferkamp et al., 2004; Vogeli et al., 2006). Furthermore, ECs and hematopoietic cells initially share expression of many genes, including *Etv2/ets1-related protein* (Sumanas and Lin, 2006), *fli1a*, *lmo2*, *gata2* (Thompson et al., 1998) and *tal1* (Gering et al., 1998). Additionally, some mouse gene knockouts (e.g. Flk1 (Shalaby et al., 1995), Etv-2 (Lee et al., 2008)) as well as zebrafish mutants *cloche* (Reischauer et al., 2016; Stainier et al., 1995) and *mirinay* (Jin et al., 2007) result in disappearance of ECs and hematopoietic cells.

In the zebrafish embryo, ECs and primitive hematopoietic cells become specified within the lateral plate mesoderm (LPM), with the anterior LPM giving rise to ECs and macrophages and the posterior LPM to ECs and primitive erythrocytes. ECs are specified once they express the *vascular endothelial growth factor receptor (vegfr) 2* ortholog *kdrl*, while primitive hematopoiesis is regulated and indicated

* Corresponding author at: University of Muenster, Roentgenstrasse 20, D-49149 Muenster, Germany.
E-mail address: wiebke.herzog@uni-muenster.de (W. Herzog).
[1] Authors contributed equally.

http://dx.doi.org/10.1016/j.ydbio.2017.08.004
Received 22 February 2017; Received in revised form 3 August 2017; Accepted 3 August 2017
Available online 12 August 2017

by the expression of *pu.1* in macrophages (anterior LPM) and of *gata1* in erythrocytes (posterior LPM) (Jagannathan-Bogdan and Zon, 2013). Within the posterior LPM, specification of *kdrl*-positive ECs and *gata1*-positive erythrocytes can be observed from 11.5 h post fertilization (hpf) or 4–5 somite stage (ss) onwards in two parallel stripes along the anterior-posterior axis (Long et al., 1997). From 14 hpf both cell populations migrate in close association towards the midline, where ECs form the major axial vessels (Helker et al., 2015). It was suggested previously, that Notch signaling negatively regulates the EC number while promoting generation of primitive erythrocytes and thereby acts as molecular switch during cell fate specification (Lee et al., 2009). However, regulators promoting EC specification from multipotent progenitors have not been identified.

β-catenin dependent Wnt signaling regulates numerous processes in the developing vertebrate embryo (Clevers and Nusse, 2012; Loh et al., 2016). During gastrulation, it has been shown to be necessary for mesoderm induction (Liu et al., 1999; Martin and Kimelman, 2012). For β-catenin dependent signaling, binding of a Wnt ligand to Frizzled receptors results in disassembly of the Axin/Gsk3β/CkI/Apc destruction complex and thereby enables accumulation of β-catenin and translocation into the nucleus. As a result, β-catenin can bind to transcription factors of the Tcf/Lef family (TCF1/Tcf7, TCF3a/Tcf7l1a, TCF3b/Tcf7l1b, TCF4/Tcf7l2 and LEF1/Lef1) and induce target gene transcription (Angers and Moon, 2009; Behrens et al., 1996). One of the universal Wnt signaling target genes is *axin2* (Leung et al., 2002). Axin2 acts in a negative Wnt signaling feedback loop, as it stabilizes the destruction complex and therefore mediates β-catenin degradation (Behrens et al., 1998). Wnt signaling has been shown to regulate angiogenic blood vessel growth and remodeling (Franco et al., 2009; Reis and Liebner, 2013; Vanhollebeke et al., 2015). But until today, the commitment of Wnt signaling to vasculogenesis has not been elucidated.

In this study we have investigated the role of β-catenin dependent Wnt signaling during EC specification in the developing zebrafish embryo and human embryonic stem (ES) cell differentiation. Our results show for the first time, that ECs specify from Fli1a-positive progenitor population in a Wnt3a-dependent manner via Lef1.

2. Materials and methods

2.1. Zebrafish husbandry and transgenic lines

Zebrafish (*Danio rerio*) embryos were maintained under standard husbandry conditions at 28.5 °C (Westerfield, 1993). Zebrafish lines used were: *Tg(etv2:GFP)*^{ci1} (Proulx et al., 2010), *Tg(fli1a:EGFP)*^{y1} (Lawson and Weinstein, 2002), *Tg(fli1a:dsRed)*^{um13} (Covassin et al., 2009), *Tg(gata1:EGFP)*^{la781} (Long et al., 1997), *Tg(gata1:dsRed)*^{sd2} (Traver et al., 2003), *Tg(hsp70l:dkk1-GFP)*^{w32} (Stoick-Cooper et al., 2007) (referred as *hs:dkk1*), *Tg(hsp70l:wnt8-GFP)*^{w34} (Weidinger et al., 2005) (referred as *hs:wnt8*), *Tg(kdrl:EGFP)*^{s843} (Jin et al., 2005), *Tg(kdrl:mCherry)*^{s896} (Chi et al., 2008) and zebrafish mutants used were *lef1*^{u767} (Valdivia et al., 2011) and *clo*^{m39} (Stainier et al., 1995).

2.1.1. Generation of transgenic fish

Tg(axin2$_{BAC}$*:Venus-Pest)*^{mu288} is based on recombining a Kozak sequence and the Venus-Pest sequence (Aulehla et al., 2008) at the start codon of the *axin2* gene into the BAC clone CH211-66B14 (196 kb) according to the previously described protocol (Bussmann and Schulte-Merker, 2011). For *Tg(14TCF:loxP-STOP-loxP-dGFP)*^{mu202}, two tandem sequences of the 7TCF-BAT promoter motif (Maretto et al., 2003) were cloned upstream of a floxed STOP cassette (loxP-STOP-loxP (Hesselson et al., 2009)) followed by destabilized GFP (dGFP (Dorsky et al., 2002)) in pTol2Dest (Villefranc et al., 2007). The *Tg(fli1a:cre)*^{mu225} line was generated by cloning the Cre recombinase gene downstream of the *fli1a* promoter using pTol2fli1epDest (Villefranc et al., 2007). Specificity of Cre expression and recombination efficiency was tested by *in situ* hybridization and mating to recombination reporter lines. Transgenesis was performed as previously described (Helker et al., 2013).

2.2. Microinjections

Morpholino (MO) - microinjections were performed as previously described (Nasevicius et al., 2000). Translation blocking MOs used in this study: *lef1* 5'-CTCCTCCACCTGACAACTGCGGCAT (Dorsky et al., 2002), 2.5 ng injected a single-cell stage; *tcf7* 5'-TGCGGCATGATCCAAACTTTCTCAA, 8 ng injected, *tcf7l1a* 5'-CCTCCTCCGTTTAACTGAGGCATGT, 8 ng injected; *tcf7l1b* 5'-GGGCTTGTCTTGCAAACGGTCACAA, 5 ng injected; *tcf7l2* 5'-CTGCGGCATTTTTCCCGAGGAGCGC, 8 ng injected; *wnt3* 5'-GATCTCTTACCATTCGTCCTGC (Mattes et al., 2012), 8 ng injected; *wnt3a* 5'-GTTAGGCTTAAACTGACACGCACAC (Buckles et al., 2004), 8 ng injected; *wnt8* 5'-ACGCAAAAATCTGGCAAGGGTTCAT and 5'-GCCCAACGGAAGAAGTAAGCCATTA (Lekven et al., 2001), co-injection of 8 ng.

For Cre recombinase expression, the *cre* coding sequence (Hesselson et al., 2009) was cloned into pCS2+ and transcribed into mRNA using the SP6 mMessage mMachine Kit (Ambion). 2 nL of *cre* mRNA (200 ng/μL) were injected at single cell stage.

For transient CRISPR-Cas9 mediated knockdown, annealed template oligonucleotides were transcribed into gRNAs using MEGAshortscript T7 Kit (Ambion)**:** *wnt3a* 5'-AAAGCACCGACTCGGTGCCACTTTTTCAAGTTGATAACGGACTAGC-CTTATTTTAACTTGCTATTTCTAGCTCTAAAACCCGCCAGAGACCTG-CAGACACCCTATAGTGAGTCGTATTACGC, *cldn5b* (used as control) 5'-AAAGCACCGACTCGGTGCCACTTTTTCAAGTTGATAACGGACTAGC-CTTATTTTAACTTGCTATTTCTAGCTCTAAAACGGTGACGGTCAAGC-AGAGTCCTATAGTGAGTCGTATTACGC. 2 nL of 500 ng/μL gRNA and 300 ng/μL *nls-zCas9-nls* mRNA (Jao et al., 2013) were injected at single cell stage. Genotyping was performed by PCR amplification using *wnt3a* fwd 5'-CCTGTTCCTTTTTTGTGGG, *wnt3a* rev 5'-GAAACTGATGCTGACACTCCTG and consecutive PstI digest (ON, 37 °C). Digested PCR fragments were analyzed by gel electrophoresis on a 4% TBE-agarose gel. We used NCBI blast to check specificity of the gRNAs and controlled efficiency of the cutting by genotyping 10 pooled embryos.

2.3. Pharmacological and heatshock treatments

Dechorionated zebrafish embryos were incubated from 9 hpf to 18.5 hpf in either 20 μM IWR-1 (Chen et al., 2009), 1 μM BIO (Gore et al., 2011; Meijer et al., 2003) or a combination of 150 μM Aphidicolin and 20 mM Hydroxyurea (AHU). For heatshock induced gene expression, embryos were incubated for 45 min in 39 °C E3 medium at 11 and 13 hpf and analyzed at 18.5 hpf.

2.4. Immunohistochemistry

Immunohistochemistry was performed as described previously (Blum et al., 2008) using rabbit anti–red fluorescent protein (ABIN129578), rabbit anti-GFP-Alexa Fluor 488 conjugated (Invitrogen) and goat anti-rabbit Atto-594 (Sigma-Aldrich).

2.5. Image acquisition and quantification of fluorescent reporter expression (volume) and cell numbers

Fluorescence images were acquired as 3D confocal stacks of the whole tail region of GFP (Leica Sp5 DM 6000 upright) and dGFP or Venus-Pest (ZEISS LSM780 inverted) expressing embryos as previously described (Hamm et al., 2016). Volume quantification of the

GFP signal was done using the volume rendering function of Imaris (Bitplane).

For analysis of cell numbers, embryos were fixed in 4% PFA overnight, washed in PBS supplemented with 0.1% Tween-20 and embedded in 4% low melting agarose (Roth). 200 µm thick transversal sections at the level of the 10–12th somite were stained with anti-GFP antibody and TOPRO-3 iodide/PBST (1 mM in DMSO, Invitrogen) to visualize nuclei, as described (Lee et al., 2009).

Statistical analysis was performed using Prism 6 (GraphPad) and p-Values were calculated by student's *t*-test and ANOVA as indicated for each experiment. Statistical significance was shown by * $p < 0.05$, ** $p < 0.01$ and *** $p < 0.001$.

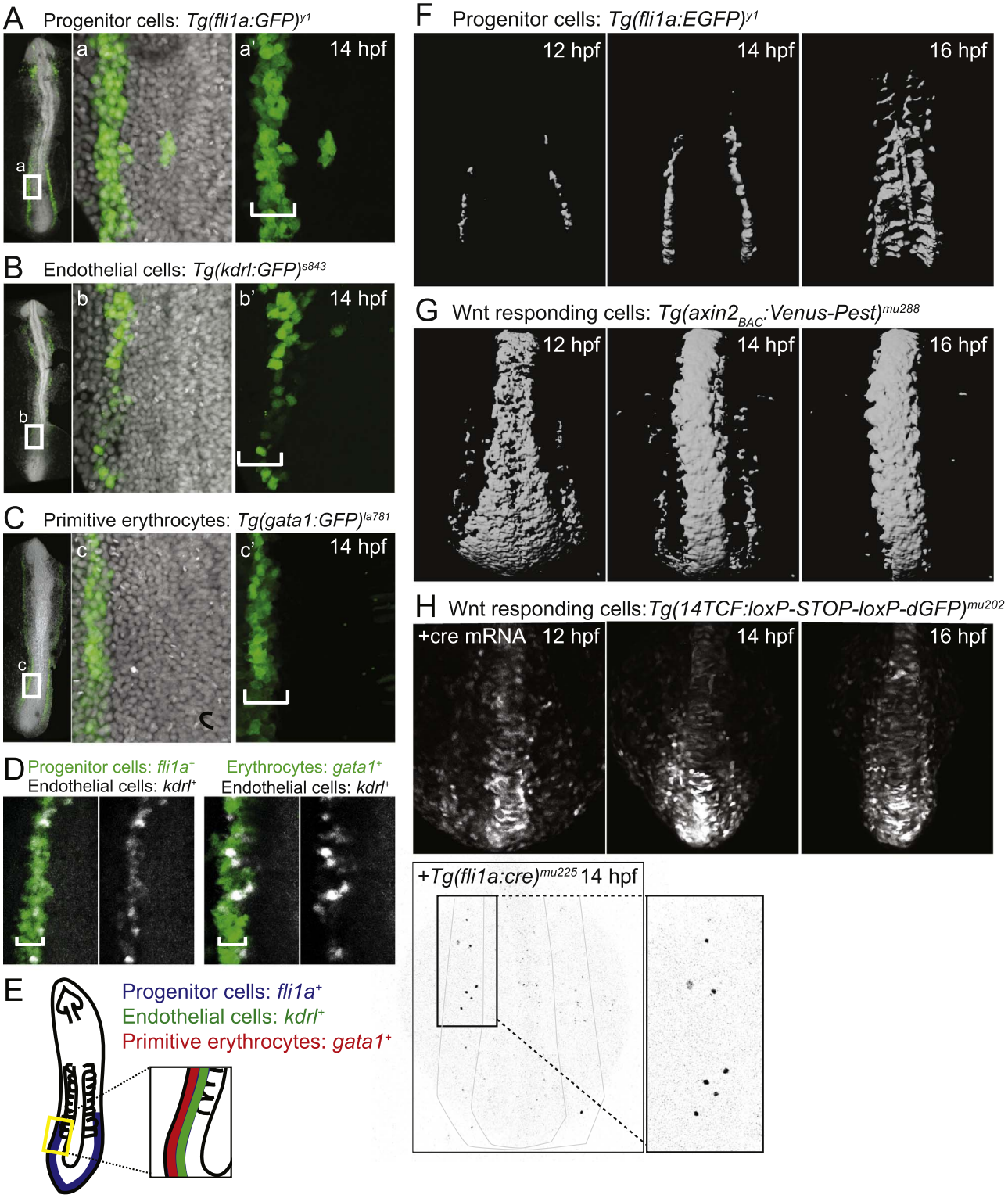

2.6. Whole mount RNA in situ hybridization (WISH)

Single and double non-fluorescent WISH (Herzog et al., 2003; Thisse and Thisse, 2008) and double fluorescent WISH (Schoenebeck et al., 2007) were performed as previously described. Embryos were cleared after staining either using benzylbenzoate: benzylalcohol (2:1) (single non-fluorescent WISH), or 80% glycerol (double non-fluorescent WISH). Templates for antisense probes were amplified from cDNA of 24 hpf old embryos using: *axin2* fwd 5'-GCCTGTTCAGAATGGCAGTT, *axin2* rev 5'-GTTCCTGTGCAATGTCTGGA; *fli1a* fwd 5'-AACGCAAGAGCAAACCCAAC, *fli1a* rev 5'-GGAAGCTTTCACATCCTGAC; *lef1* fwd 5'-TATCTCGGGAAGAGCAAGCT, *lef1* rev 5'-TACAGAGGAAAAGTGACATCC; *venus* fwd 5'-CAAGGGCGAGGAGCTGTT, *venus* rev 5'-TGATCCTAGCAGAAGCACAGG; *wnt3a* fwd 5'-TGTGTAGCTCAATTCCTGGC, *wnt3a* rev 5'-ACTTGCAGGTGTGAACATCG. *lef1* and *wnt3a* cDNA fragments were cloned into pGEM-T Easy (Promega) and antisense probes were synthesized using T7 (*axin2, lef1, venus*) or Sp6 promoter (*wnt3a*). The antisense *axin2*, *fli1a* and *venus* probes were synthesized using a T7 promoter containing reverse primer in an additional amplification step: T7-axin2 rev 5'-AACGTAATACGACTCACTATAGGGAAGTTCCTGTGCAATGTCTGGA; T7-*fli1a* rev 5'-AACGTAATACGACTCACTATAGGGGGAAGCTTTCACATCCTGAC; T7-venus rev 5'- AACGTAATACGACTCACTATAGGGAATGATCCTAGCAGAAGCACAGG. The antisense *GFP* and *tal1* probes were generated as described (Moro et al., 2012; Thisse and Thisse, 2008).

2.7. Differentiation of human ES cells

Human ES cells (line HuES6) were cultured under feeder-free conditions in chemically defined FTDA medium (Frank et al., 2012). Following dissociation into single cells using Accutase, ES cells were seeded at 500,000 cells per well of a Matrigel-coated 24-well plate into mesoderm induction media containing KODMEM (Life Technologies), Insulin/Transferrin/Selenium (BD), PenStrep/Glutamine, 10 μM Y-27632, 2 μM CHIR 99021 (Santa Cruz), 2 ng/ml BMP4 (R & D Systems) and 20 ng/ml FGF2 (R & D Systems). On the next day, medium was changed to KO-DMEM, Transferrin/Selenium (BD), PenStrep/Glutamine, 2 μM CHIR 99021, 2 ng/ml BMP4 and 20 ng/ml FGF2. On day 2 and 3, cells were either treated with 1 μM CHIR 99021 alone (Blaschke et al., 2013), 2 μM IWP-2 (Chen et al., 2009) (Santa Cruz), or kept untreated. Hence after, cells were further cultured in basal differentiation medium without growth factors / inhibitors as indicated in figures. Gene expression was either analyzed in a time-course fashion using Illumina human-12 microarrays or at day 10 of differentiation using RT-qPCR or immunocytochemistry.

2.8. Microarray, RT-qPCR, Immunocytochemistry

Cells were directly lysed on culture dishes and RNA was extracted using RNeasy Mini kits with on-column DNA digestion (Qiagen). For analysis on Illumina HumanHT-12 v4 microarrays, cRNA was prepared and samples hybridized and analyzed as described elsewhere (Greber et al., 2011). For RT-qPCR, 1 μg of total RNA was reverse transcribed using MMLV Reverse Transcriptase (USB #78306) and oligo-dT priming following the manufacturer's instructions. Real-time PCR was performed using validated primer pairs listed in Table S1 and iTaq SYBR Green Supermix with ROX (Bio-RAD) on ABI Prism 7500 instrumentation. Fold mRNA expression changes were determined using the ΔΔCt method based on normalization against RPL37A. Data were averaged from three biological replicates. Student's *t*-tests were performed to reveal statistical significance against IWP-2 treated samples. Immunocytochemistry was performed using PECAM1 (R & D #BBA7) and Alexa-488 conjugated secondary antibodies.

3. Results

3.1. ECs and primitive erythrocytes derive from a common progenitor population at the posterior lateral plate mesoderm

ECs and primitive erythrocytes originate from the same progenitor population (Brown et al., 2000; Haferkamp et al., 2004; Liu et al., 2008). In zebrafish, *fli1a* is used as a marker for this multipotent progenitor cells (Brown et al., 2000; Liu et al., 2008). We detected these progenitor cells using *Tg(fli1a:GFP)* in bilateral stripes in lateral plate mesoderm at 14 hpf (Fig. 1A). At this stage, ECs expressing *Tg(kdrl:GFP)* and primitive erythrocytes expressing *Tg(gata1:GFP)* localize to the same region in the zebrafish embryo (Fig. 1B,C). Higher magnification revealed, that the *fli1a*-positive cell population in posterior LPM has a width of about 30 μm consisting of five to six cells (Fig. 1A inlet a). Within the same region, the EC population has a width of one to two cells, which are positioned more medially within the *fli1a*-positive progenitor cell population (Fig. 1B inlet b). In contrast, the primitive erythrocytes occupy a width of three to four cells, which were positioned in the lateral part of the progenitor cell population (Fig. 1C inlet c). We confirmed by immunofluorescence staining of double transgenic fish expressing either *fli1a:dsRed* and *kdrl:GFP* or *gata1:dsRed* and *kdrl:GFP*, that *kdrl*-positive ECs occupy the medial part of the *fli1a*-positive progenitor cell population (Fig. 1D).

Therefore, at 14 hpf in the anterior most region of the posterior LPM we identify a spatial subdivision of ECs and primitive erythrocytes within the *fli1a*-positive progenitor cell population, with ECs localizing to the medial and erythrocytes localizing to the lateral part of the posterior LPM (Fig. 1E).

3.2. β-catenin dependent Wnt signaling is active in a subset of the fli1a-positive cell population

To analyze *in vivo* if the *fli1a*-positive progenitor cells display active Wnt signaling during specification of ECs and primitive erythrocytes, we generated novel Wnt reporter transgenic zebrafish lines, expressing destabilized fluorophores under the control of Wnt responsive promoters (Fig. 2). Therefore, we generated a transgenic zebrafish line expressing a very short-lived Venus (Venus-Pest (Aulehla et al., 2008)) downstream of the natural *axin2* promoter, which was cloned using BAC recombination of the full-length promoter sequence. We

Fig. 1. Wnt signaling is active in the *fli1a*-positive progenitor cell population of the posterior LPM, consisting of medial *kdrl*-positive cells and more lateral *gata1*-positive cells. (A-D) Position of the progenitor cell population (A, *Tg(fli1a:GFP)^{y1}*), endothelial cells (B, *Tg(kdrl:GFP)^{s843}*, ECs) and erythrocytes (C, *Tg(gata1:GFP)^{la781}*) in the posterior LPM at 14 hpf (10ss). (a-c, a'-c') Magnified dorsal images of the left side of the posterior LPM region caudal to the 9th somite. Scale bars 30 μm. The *fli1a*-positive cell population has a width of 4–5 cells (A), the *kdrl*-positive cell population has a width of 1–2 cells (B) and the *gata1*-positive cell population has a width of 3–4 cells (C). Double labeling of *fli1a*-positive and *kdrl*-positive cells (D, left panel, *Tg(kdrl:GFP)^{s843};(fli1a:dsRed)^{y1}* with immuno-labeling of dsRed) or of *gata1*-positive erythrocytes and *kdrl*-positive ECs (D, right panel, *Tg(kdrl:GFP)^{s843};(gata1:dsRed)^{sd2}* with immuno-labeling of dsRed) indicated, that *kdrl*-positive ECs are sorted more medially within the *fli1a*-positive cell population than *gata1*-positive cells. (E) Schematic of the posterior LPM at 14 hpf illustrating the localization of the *kdrl*-positive (ECs, green) and the *gata1*-positive (erythrocytes, red) cell populations within the *fli1a*-positive progenitor cell population (purple) as shown in A-D. (F-H) Time course of the migration of *fli1a*-positive cells from 12 to 16 hpf. Dorsal views of the posterior LPM. Images were processed either as surface rendering projections (F,G) or displayed as maximum intensity projections (H, upper panel) or using inverted colors (H, lower panel) for better visualization. *Tg(fli1a:GFP)^{y1}* is expressed in bilateral stripes that migrate towards the midline (F). Wnt responding cells from *Tg(axin2$_{BAC}$:Venus-Pest)^{mu288}* (G) or *cre* mRNA injected *Tg(14TCF:loxP-STOP-loxP-dGFP)^{mu202}* (H, upper panel) show mesodermal expression in the developing somites and expression in bilateral stripes similar to *Tg(fli1a:GFP)^{y1}*. Double transgenic embryos for *Tg(14TCF:loxP-STOP-loxP-dGFP)^{mu202}* and *Tg(fli1a:cre)^{mu225}* exhibit GFP expression in a subset of *fli1a*-positive cells at 14 hpf (H, lower panel). Grey lines surround the region of the migrating *fli1a*-positive cell population.

observed Venus-Pest expression not only in the mesoderm of the developing somites, but also in bilateral stripes of the posterior LPM, which seems to correspond to similar positions as *Tg(fli1a:GFP)* at 12 hpf (Fig. 1 F,G). Comparable to the *fli1a*-positive cell population, these Venus-Pest positive cells migrate to the midline between 12 and 16 hpf (Fig. 1 F,G).

As an alternative reporter for β-catenin dependent Wnt signaling, we used the well-established approach of combining synthetic TCF binding sites with a minimal promoter (Maretto et al., 2003; Moro et al., 2012; Shimizu et al., 2012). To generate a line which can also be used to report tissue specific Wnt response, we engineered 14 TCF binding sites (14TCF) before a loxP-flanked STOP cassette (Hesselson et al., 2009), driving expression of a destabilized GFP (dGFP, (Dorsky et al., 2002)), called *Tg(14TCF:loxP-STOP-loxP-dGFP)*^{mu202}. Following injection of *cre* mRNA into *Tg(14TCF:loxP-STOP-loxP-dGFP)*^{mu202} embryos at single cell stage, and thereby excising the STOP cassette in all cells, we could detect GFP expression in bilateral stripes that migrate to the midline in addition to the mesodermal expression domain in the medial mesoderm similar to *Tg(axin2*$_{BAC}$*:Venus-Pest)*^{mu288} (Fig. 1H, upper panel).

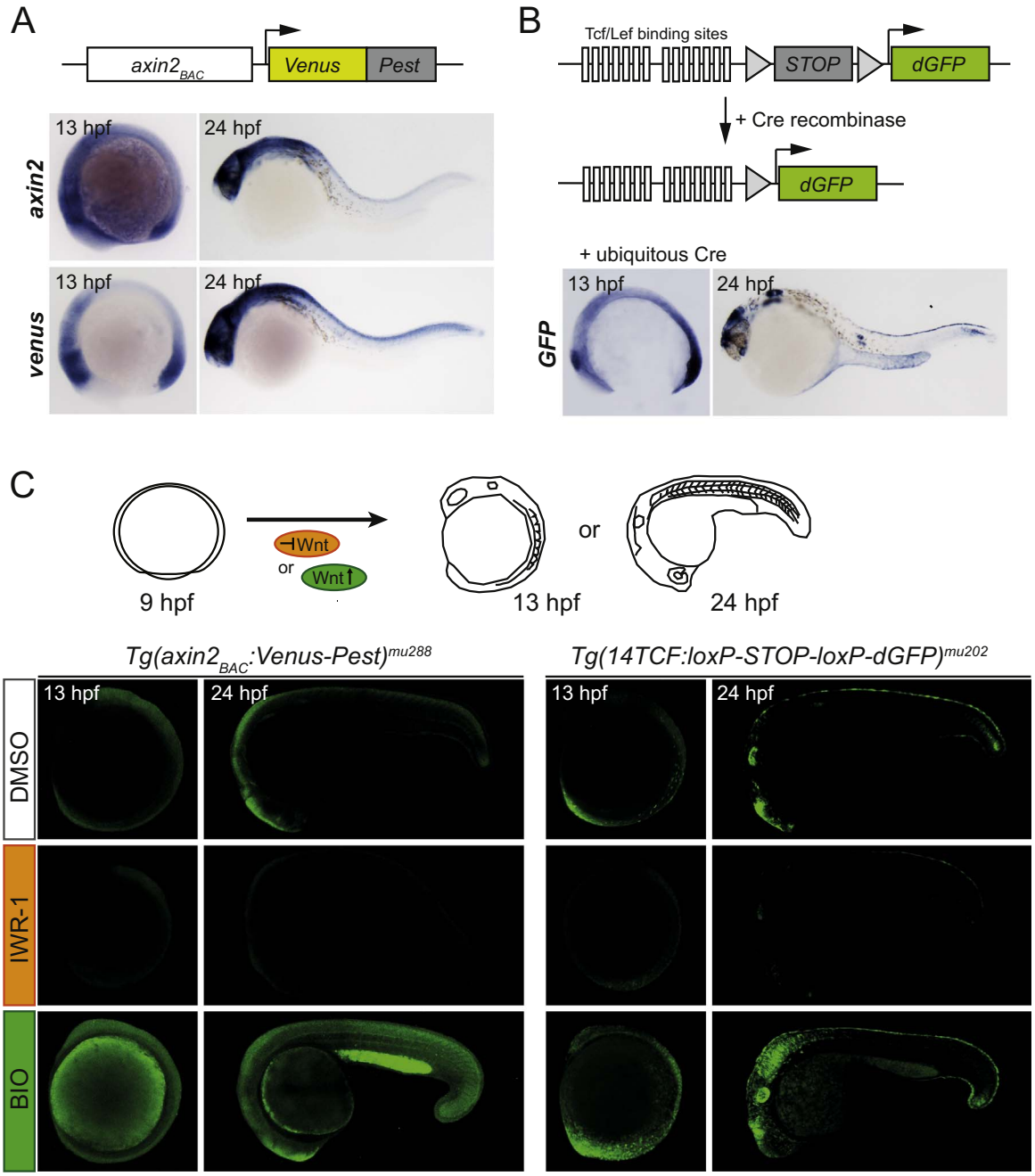

Fig. 2. *Tg(axin2*$_{BAC}$*:Venus-Pest)*^{mu288} and *Tg(14TCF:loxP-STOP-loxP-dGFP)*^{mu202} lines represent *bona fide* β-catenin dependent Wnt signaling reporters. (A,B) Domain structure of Tg(*axin2*$_{BAC}$*:Venus-Pest)*^{mu288} (A) and *Tg(14TCF:loxP-STOP-loxP-dGFP)*^{mu202} (B), and whole mount *in situ* hybridization using antisense *axin2, Venus* and *GFP* probes. *axin2* and *Venus* and *GFP* are expressed in similar domains: at 13 hpf hindbrain-midbrain boundary, posterior neuroectoderm and mesoderm; at 24 hpf in parts of the developing CNS, the skin and slightly in the tail tip with the GFP expression at 24hpf being limited to smaller domains in the CNS. (C) *Tg(axin2*$_{BAC}$*:Venus-Pest)*^{mu288} (left panel) and *Tg(14TCF:loxP-STOP-loxP-dGFP)*^{mu202} (right panel) embryos were exposed to a Wnt signaling inhibitor (IWR-1) or a Wnt signaling activator (BIO) from 9 to 13 hpf or to 24 hpf and analyzed by confocal microscopy. Treatment with IWR-1 strongly reduced the fluorescence signal of both reporter lines compared to DMSO controls. *Vice versa*, treatment with Wnt signaling activator BIO resulted in strongly increased expression of both reporters compared to the respective controls. Hence, Tg(*axin2*$_{BAC}$*:Venus-Pest)*^{mu288} and *Tg(14TCF:loxP-STOP-loxP-dGFP)*^{mu202} faithfully respond to Wnt signaling stimulation. For analysis, *Tg(14TCF:loxP-STOP-loxP-dGFP)*^{mu202} embryos were injected with *cre* mRNA at single cell stage.

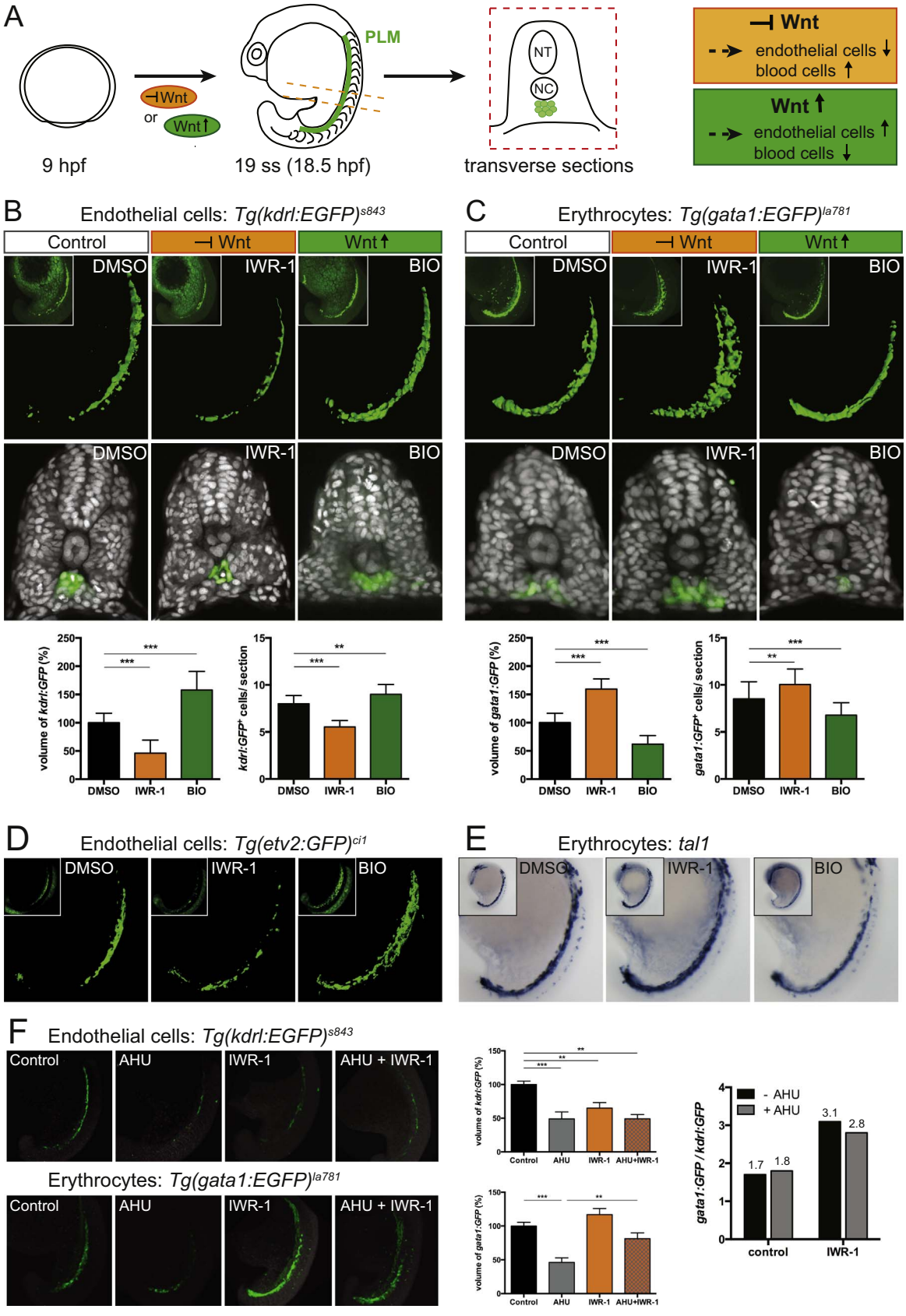
A
PLM
Wnt
or
Wnt↑
NT
NC
9 hpf
19 ss (18.5 hpf)
transverse sections
Wnt
endothelial cells ↓
blood cells ↑
Wnt↑
endothelial cells ↑
blood cells ↓
B
Endothelial cells: Tg(kdrl:EGFP)s843
C
Erythrocytes: Tg(gata1:EGFP)la781
Control
Wnt
Wnt↑
DMSO
IWR-1
BIO
volume of kdrl:GFP (%)
kdrl:GFP+ cells/ section
volume of gata1:GFP (%)
gata1:GFP+ cells/ section
D
Endothelial cells: Tg(etv2:GFP)ci1
E
Erythrocytes: tal1
F
Endothelial cells: Tg(kdrl:EGFP)s843
Erythrocytes: Tg(gata1:EGFP)la781
Control
AHU
IWR-1
AHU + IWR-1
volume of kdrl:GFP (%)
volume of gata1:GFP (%)
gata1:GFP / kdrl:GFP
- AHU
+ AHU
1.7
1.8
3.1
2.8
control
IWR-1

To excise the STOP cassette in the *fli1a*-positive progenitor cell population we generated transgenic zebrafish, expressing Cre recombinase under the control of the *fli1a* promoter, called *Tg(fli1a:cre)*^{mu225}. In *Tg(fli1a:cre*; *14TCF:loxP-STOP-loxP-dGFP*) double transgenic embryos we detected Wnt reporter expression in a small cell population (Fig. 1 H, lower panel). This clearly demonstrates the Wnt activity within some *fli1a*-positive cells. However, our careful analysis of the *Tg(fli1a:cre)* line indicated that we could not target all *fli1a*-positive cells using this line, therefore resulting in fewer Wnt signaling positive cells than expected.

We validated our novel Wnt signaling reporters by comparing the endogenous *axin2* expression with reporter driven expression as well as by pharmacological Wnt signaling inhibition or stimulation (Fig. 2A-C).

In sum, by using our two Wnt signaling reporter strains, we could show that Wnt signaling is active in a subset of the *fli1a*-positive cell population during the time window of EC and primitive erythrocyte specification.

3.3. β-catenin dependent Wnt signaling promotes EC specification, while negatively regulating primitive erythrocyte specification

With β-catenin dependent Wnt signaling being active in the *fli1a*-positive progenitor population, we analyzed its functional consequences. Therefore, we pharmacologically manipulated Wnt signaling using inhibitor of Wnt response 1 (IWR-1, (Chen et al., 2009)) and the Wnt signaling activator BIO (Gore et al., 2011; Meijer et al., 2003). Both agents act on components of the β-catenin destruction complex and thereby regulate β-catenin availability: treatment with IWR-1 reduces cytosolic β-catenin by stabilizing Axin2 in the destruction complex, whereas treatment with BIO increases the cytosolic pool of β-catenin through inhibition of GSK3β. We treated zebrafish embryos prior to EC specification (at 9 hpf) continuously until 18.5 hpf (19 ss), when specified ECs have migrated to the midline, but did not yet form a vessel (Fig. 3A). We analyzed EC specification by quantifying the total volume of the *kdrl*-expressing cell population using *Tg(kdrl:GFP)*^{s843} embryos, or by counting GFP-positive EC nuclei in transversal sections (Fig. 3B). Inhibition of Wnt signaling by IWR-1, led to a significant decrease in the total EC volume of 46% compared to control and reduced the number of GFP-positive ECs (IWR-1: 5.5 ± 0.6 cells, DMSO: 8.0 ± 0.8 cells; Fig. 3B). In contrast, activation of Wnt signaling using BIO, increased the total volume of *kdrl:GFP* to 158% compared to control and elevated the cell number of GFP-positive ECs (BIO: 9.1 ± 0.9 cells, Fig. 3B). We observed similar effects of Wnt signaling manipulation when analyzing the ECs by GFP expression from *Tg(etv2:GFP)*^{ci1} positive embryos (Fig. 3D). Our data strongly indicate that β-catenin dependent Wnt signaling positively regulates EC number and expands the EC population.

In the posterior LPM ECs and primitive erythrocytes are being specified in close proximity (Fig. 1A-C). We therefore analyzed whether β-catenin dependent Wnt signaling also influences erythrocyte specification. We inhibited or stimulated Wnt signaling in an erythrocyte specific transgenic line (*Tg(gata1:GFP)*^{la781}) and measured GFP volume. Interestingly, inhibition of Wnt signaling by IWR-1 significantly increased the total volume of *gata1:GFP* to 160% compared to DMSO treated embryos and raised the cell number of GFP-positive erythrocytes (IWR-1: 10 ± 1.6 cells, DMSO: 8.5 ± 1.8 cells; Fig. 3C). Activation of Wnt signaling by BIO had the opposite effect and reduced total volume of *gata1:GFP* to 62% and decreased cell number of GFP-positive erythrocytes (BIO: 6.8 ± 1.3 cells; Fig. 3C). We additionally showed similar effects of Wnt manipulation on the erythrocytes by detecting *tal1* expression using whole mount *in situ* hybridization (Fig. 3E).

Previously, Wnt signaling has been shown to affect fate of cell populations by regulating asymmetric cell division (Habib et al., 2013; Ouspenskaia et al., 2016). In order to test, whether Wnt signaling regulates EC versus erythrocyte specification from progenitor cells through asymmetric cell division, we treated zebrafish embryos with a proliferation inhibitor cocktail (aphidicolin and hydroxyurea, AHU) and analyzed the differentiation into ECs or erythrocytes as before. Treatment of embryos with AHU from 9 hpf to 18.5 hpf efficiently blocked cell proliferation and reduced the total volume of both ECs (*kdrl:GFP* positive) and erythrocytes (*gata1:GFP* positive) compared to control to about 50% (Fig. 3F). However, when we determined the ratio between specified erythrocytes and ECs, there was no alteration through block of proliferation (Fig. 3F). During unperturbed development we observed a volume ratio of GFP-positive erythrocytes and ECs of 1.7, which remained 1.8 after block of proliferation. In contrast, single or co-treatment with Wnt inhibitor IWR-1 increased the *gata1:GFP/kdrl:GFP* ratio in comparison to control (IWR-1: 3.1, IWR-1+AHU: 2.8; Fig. 3F).

We therefore conclude, that while β-catenin dependent Wnt signaling positively regulates EC specification, this does not require cell division.

3.4. Wnt3a positively regulates EC specification during somitogenesis

To identify the specific Wnt ligand that regulates EC specification, we screened for expression of the 15 potential canonical Wnt ligands at 12 hpf by *in situ* hybridization (*wnt1, wnt2, wnt2ba, wnt2bb, wnt3, wnt3a, wnt4a, wnt8a, wnt8b, wnt8like, wnt9a, wnt9b, wnt10a, wnt10b* and *wnt16*; data not shown). We selected the ligands that were expressed in the LPM and used antisense morpholino-oligonucleotides (MO) to abolish translation. We again counted the number of ECs in transversal sections and measured the posterior EC volume in *Tg(kdrl:GFP)* embryos. MO-mediated knockdown of *wnt9a*, *wnt9b*, *wnt8* or *wnt3* had no effect on the EC number (Fig. 4A). However, Wnt3a deficiency reduced the number of ECs to the same level as IWR-1 treatment (*wnt3a* MO: 5.7 ± 0.9 cells, ctr. MO: 8.4 ± 0.8 cells; Fig. 4A,B, compare to Fig. 3B). Likewise, the total volume of ECs was significantly reduced after

Fig. 3. β-catenin dependent Wnt signaling positively regulates the number of ECs, while negatively regulating the number of erythrocytes. (A) Schematic representation of the experiment. (B) EC volume and cell numbers were analyzed by GFP expression in *Tg(kdrl:GFP)*^{s843} embryos. (C) Erythrocyte volume and cell numbers were analyzed by GFP expression in *Tg(gata1:GFP)*^{la781} embryos. Confocal images with the insets representing the overview, and the larger images displaying the specific volume used for quantification. Nuclei were visualized using TOPRO-3 (white). Inhibition of Wnt signaling by IWR treatment led to a reduction in EC volume (B, n = 10) and EC cell numbers (B, n = 19), and to an increase in erythrocyte volume (C, n = 6) and erythrocyte cell numbers (C, n = 22) compared to DMSO treated control embryos (volumes: B, n = 11; C, n = 8; cell numbers: B, n = 30; C, n = 25). Wnt activation (BIO) increased the EC volume (B, n = 8) and the EC number (B, n = 10), while decreasing the erythrocyte volume (C, n = 8) and the erythrocyte number (C, n = 36) compared to DMSO treated control embryos. Values represent mean ± SD. *p < 0.05, **p < 0.01, ***p < 0.001; Student's *t*-test. (D,E) Alternative analysis of the EC population by GFP expression of *Tg(etv2:GFP)*^{ci1} (D) and of the erythrocyte cell population using whole mount *in situ* hybridization with an antisense *tal1* probe (E). As observed by *kdrl* or *gata1* expression (B,C), Wnt inhibitor treatment (IWR-1) resulted in reduced EC volume, but in an expanded erythrocyte cell population. Treatment with Wnt activator (BIO) increased the EC volume and decreased the erythrocytes population, respectively. Note, that for EC volume analysis of *Tg(etv2:GFP)*^{ci1} the GFP staining in the muscle tissue was cropped and not included in the analysis. (F) Analysis of the EC volume using *Tg(kdrl:GFP)*^{s843} and erythrocyte volume using *Tg(gata1:GFP)*^{la781} in embryos treated with either Wnt inhibitor (IWR-1), proliferation inhibitor (AHU) or both (AHU+IWR-1). Inhibition of proliferation by AHU decreased the volume of *kdrl:GFP* and *gata1:GFP* compared to untreated control embryos, but had no effect on the ratio of both populations (indicated as *gata1:GFP/kdrl:GFP*). Hence, Wnt signaling specifically affects cell fate specification of ECs and erythrocytes and does not act via asymmetric cell division. (F, n ≥ 8), Values represent mean ± SEM. *p < 0.05, **p < 0.01, ***p < 0.001; Student's *t*-test.

wnt3a knockdown using injection of *wnt3a* MO or a *wnt3a* targeting CRISPR-Cas9 combination (to 45–55% compared to control, Fig. 4C; compare to Fig. 3B), indicating that Wnt3a regulates EC specification in the zebrafish embryo. We further detected *wnt3a* expression in the medial mesoderm, flanked by the bilateral fli1a-positive progenitor population in the posterior LPM at 14 hpf (Fig. 5B,C). Furthermore, we used transgenic overexpression of a Wnt ligand (*Tg(hsp70l:wnt8-GFP),* referred as *hs:wnt8*) or the Wnt inhibitor Dkk1 (*Tg(hsp70l:dkk1-GFP),* referred as *hs:dkk1*) to manipulate Wnt signaling through heatshock and analyzed the EC volumes in *Tg(kdrl:mCherry)*. While overexpression of Wnt8 increased the EC volume, Dkk1 expression led to a decrease in EC volume compared to control siblings (*hs:wnt8*: 142%, *hs:dkk1*: 50%, Fig. 4F). Hence, EC specification is promoted by increased Wnt ligand availability.

3.5. Lef1 is expressed in a subset of the fli1a-positive progenitor cell population and promotes EC specification

Additionally, we wanted to identify the transcription factor transducing the specification signal. There are five different Tcf/Lef transcription factors known in zebrafish: *lef1*, *tcf7*, *tcf7l1a*, *tcf7l1b* and *tcf7l2* (Angers and Moon, 2009; Behrens et al., 1996). We performed individual MO-mediated knockdown of all five transcription factors and analyzed the EC number of *Tg(kdrl:EGFP)* embryos. We observed no significant changes after knockdown of *tcf7*, *tcf7l1a*, *tcf7l1b* or *tcf7l2* (Fig. 4D). However, knockdown of *lef1* significantly reduced the number of ECs (*lef1* MO: 4.8 ± 0.9 cells, ctr. MO: 8.0 ± 1.0 cells; Fig. 4D,E). Comparing ECs and erythrocytes, MO-mediated knockdown of *lef1* reduced the total volume of the EC population to 48% compared to control and increased to total volume of the erythrocyte population to 143%, similar to IWR-1 treatment (Fig. 4H; compare to Fig. 3B). We confirmed these data by analyzing *lef1*^{u767} mutant embryos.

Embryos carrying heterozygous and homozygous *lef1*^{u767} mutations showed reduced EC volumes, but increased erythrocyte volumes compared to wild type siblings (Fig. 4G).

Interestingly, the phenotype of overactivation of the Wnt signaling pathway by treatment with BIO, could be rescued by MO-mediated *lef1*-knockdown, indicating that Lef1 is the major downstream transcription factor, but also suggesting that other Tcf transcription factors can be activated in this process and thereby partially compensate (Fig. 4H). We therefore conclude, that Lef1 is the main transcription factor transducing the Wnt3a signal during EC specification. However, we do not exclude a minimal contribution of other Tcf family members.

To analyze *lef1* expression, we performed individual and double *in situ* hybridization for *fli1a* and *lef1*. As previously reported, *lef1* was strongly expressed in the tail bud (Fig. 5E, asterisk (Dorsky et al., 2002)). However, we also detected bilateral expression within the posterior LPM (Fig. 5E), which was narrower than the *fli1a* expression domain (Fig. 5D) and co-localized with a subset of *fli1a*-positive cells (Fig. 5F,H,I). In homozygous *cloche* mutants, lacking ECs and erythrocytes, we did not detect the bilateral expression of *fli1a* and *lef1* (Fig. 5G). We therefore assume, that *fli1a* is expressed in ECs as well as erythrocytes, but that only putative ECs are positive for *lef1* at this developmental stage.

Taken together we show, that Lef1 specifically promotes EC specification in the progenitor cell population, which receives Wnt3a stimulation most likely from the medial mesoderm.

3.6. Wnt signaling promotes EC differentiation in human ES cells

To analyze whether Wnt signaling would also promote EC fate in a mammalian system, we investigated the effects of Wnt signaling inhibition or enhancement on human mesodermal cells. We hence induced mesoderm formation in human ES cells using a cocktail of BMP, Wnt, and FGF agonists and then, 2 days later applied either Wnt stimulation (using the GSK3β inhibitor CHIR 99021), no treatment, or Wnt inhibition (by IWP-2) for another 2 days (Fig. 6A). The effects of these different treatments following mesoderm induction were analyzed on day 10. Compared to untreated samples, inhibition of Wnt signaling resulted in a significant reduction in the expression of EC markers PECAM1 and CDH5 (VE-Cadherin) by RT-qPCR (Fig. 6B). Additional Wnt stimulation only had a moderate effect on the induction of these markers, suggesting that Wnt signaling was active in these cells. The stimulatory effect of endogenous and extrinsic Wnt signaling on EC differentiation was confirmed by immunohistochemistry, whereby EC networks became apparent in untreated and Wnt stimulated samples, but not in Wnt inhibited ones (Fig. 6C).

To further elucidate whether the stimulatory effect on EC differentiation could potentially be mediated by LEF1, human ES cells were treated as before to monitor gene expression during EC specification. As a confirmation, the early primitive streak marker MIXL1 was indeed strongly upregulated by the initial exposure to the mesoderm induction factor cocktail, whereas its downregulation after day 2 appeared to be independent of Wnt signaling activity (Fig. 6D,E left panel). In contrast, LEF1 was induced upon mesoderm induction and became further upregulated if cells were left untreated, but under Wnt inhibition conditions LEF1 expression was significantly diminished (Fig. 6E right panel). These data confirm that Wnt signaling positively induces EC fate in mesodermal cells, which is in agreement with the observed expression of Lef1 in a subset of Fli1a-positive cells in the zebrafish embryo, at 14 hpf (Fig. 5D-I), following a putative earlier stimulus (by Wnt3a expression from 10 hpf on).

4. Discussion

To analyze the Wnt signaling response in the developing embryo we generated novel transgenic Wnt reporter zebrafish lines using the short-lived fluorophores dGFP and Venus-Pest as readout proteins ((Aulehla et al., 2008; Dorsky et al., 2002); see Fig. 1). While this approach resulted in much weaker reporter signals than the previously generated Wnt reporters (Dorsky et al., 2002; Moro et al., 2012; Shimizu et al., 2012), it allowed us for the first time to visualize active Wnt signaling within the Fli1a-positive progenitor cell population, which using a stable fluorophore would have been masked by previous Wnt signaling in the unspecified mesoderm. Additionally we generated novel reporter fish, which will allow us in the future to analyze tissue specific Wnt responses, based on tissue specific Cre recombinase expression.

We further showed, that Wnt3a regulates EC specification within the Fli1a-positive progenitor cell population in the developing zebrafish embryo. An alternative hypothesis, that Wnt signaling does not regulate specification, but proliferation of the EC cell population, is not supported by our data. For one, we did not observe any increase in the Fli1a-positive cell population. Secondly, inhibition of proliferation did not affect the ability of Wnt to affect EC and erythrocyte specification (Fig. 3). Interestingly, the Wnt (Wnt3a)- induced EC fate is mediated via the transcription factor Lef1, which is expressed only in a subpopulation of Fli1a-positive progenitors (Fig. 5). Lef1 expression in human ES cells as well as in zebrafish embryos points to an initial amplification loop, by which autocrine or Wnt induced upregulation of Lef1 expression would allow for higher responsiveness of *lef1*-positive cells to the medial Wnt signal (Figs. 5, 6). This is in full agreement with our observed short pulse of the fluorescent short lived Wnt reporter expression (in *Tg(axin2*$_{BAC}$*:Venus-Pest)*^{mu288} and *Tg(14TCF:loxP-STOP-loxP-dGFP)*^{mu202} embryos, Fig. 1). During specification, *kdrl*-positive ECs become sorted to a more medial position than *gata1*-positive erythrocytes (Fig. 1), presumably where they receive mesodermal Wnt signals. This cell sorting can also be seen during murine development, where progenitors of the yolksac blood islands sort into central erythrocytes surrounded by ECs, which then fuse to form a

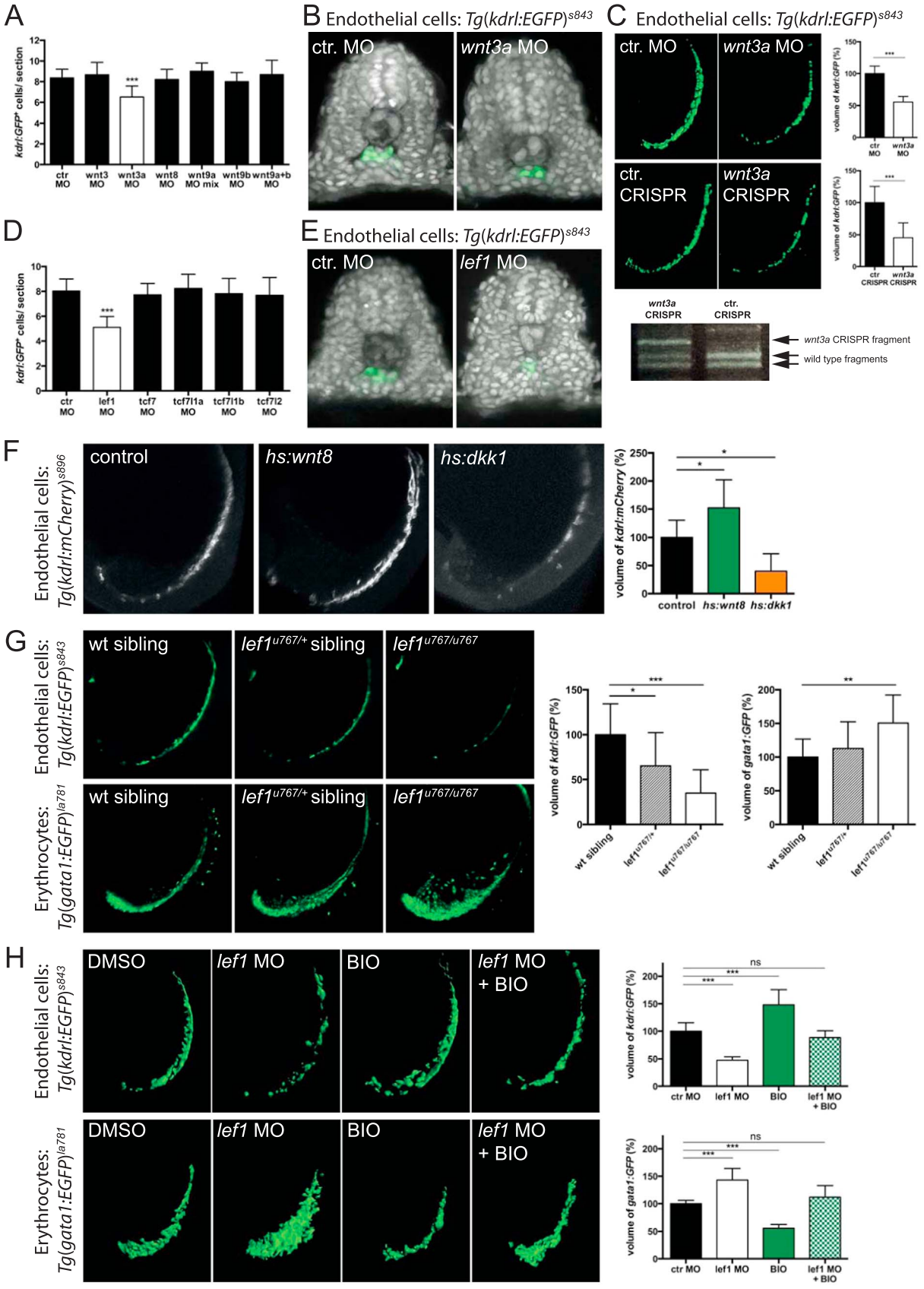
A
kdrl:GFP+ cells/ section
ctr MO
wnt3 MO
wnt3a MO
wnt8 MO
wnt9a MO mix
wnt9b MO
wnt9a+b MO
B Endothelial cells: Tg(kdrl:EGFP)s843
ctr. MO
wnt3a MO
C Endothelial cells: Tg(kdrl:EGFP)s843
ctr. MO
wnt3a MO
ctr. CRISPR
wnt3a CRISPR
volume of kdrl:GFP (%)
ctr MO
wnt3a MO
ctr CRISPR
wnt3a CRISPR
wnt3a CRISPR
ctr. CRISPR
wnt3a CRISPR fragment
wild type fragments
D
kdrl:GFP+ cells/ section
ctr MO
lef1 MO
tcf7 MO
tcf7l1a MO
tcf7l1b MO
tcf7l2 MO
E Endothelial cells: Tg(kdrl:EGFP)s843
ctr. MO
lef1 MO
F
Endothelial cells: Tg(kdrl:mCherry)s896
control
hs:wnt8
hs:dkk1
volume of kdrl:mCherry (%)
control
hs:wnt8
hs:dkk1
G
Endothelial cells: Tg(kdrl:EGFP)s843
wt sibling
lef1u767/+ sibling
lef1u767/u767
Erythrocytes: Tg(gata1:EGFP)la781
wt sibling
lef1u767/+ sibling
lef1u767/u767
volume of kdrl:GFP (%)
volume of gata1:GFP (%)
wt sibling
lef1u767/+
lef1u767/u767
H
Endothelial cells: Tg(kdrl:EGFP)s843
DMSO
lef1 MO
BIO
lef1 MO + BIO
Erythrocytes: Tg(gata1:EGFP)la781
DMSO
lef1 MO
BIO
lef1 MO + BIO
volume of kdrl:GFP (%)
volume of gata1:GFP (%)
ctr MO
lef1 MO
BIO
lef1 MO + BIO
ns

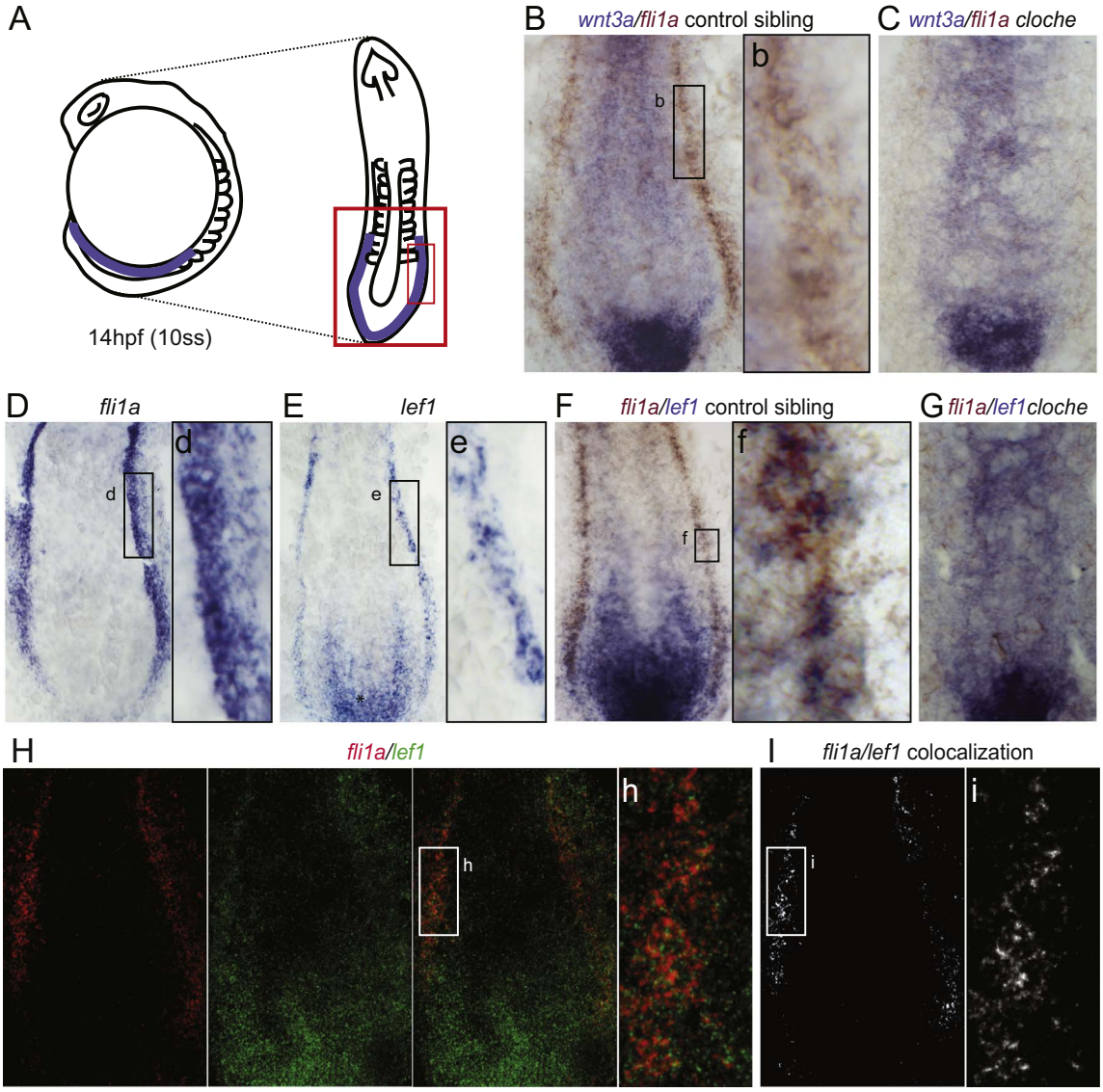

Fig. 5. *wnt3a* is expressed in the medial mesoderm, flanked by *fli1a*-positive cells, while *lef1* is expressed in a subpopulation of *fli1a*-positive cells. (A) Position of the *fli1a*-positive progenitor cell population in a 14 hpf old zebrafish embryo (blue). Left: lateral view, Right: dorsal view, with the red box at the posterior side indicating the region of analysis. (B-C) Double *in situ* hybridization for *fli1a* (red) and *wnt3a* (blue). Wild type embryos showed *wnt3a* expression in the medial mesoderm, flanked by *fli1a* expressing tissue (B, higher magnification b). In homozygous *cloche* mutant embryos lacking ECs and erythrocytes, *fli1a* expression was absent, while *wnt3a* expression could be detected in the medial mesoderm in a patchier pattern compared to the wild type siblings (C). (D-G) *In situ* hybridization for *fli1a* or/and *lef-1*. *fli1a* was expressed bilaterally in posterior LPM (D, higher magnification d). In comparison, *lef1* was also expressed bilaterally in the posterior LPM, but in a narrower region (E, higher magnification e) and additionally in the tailbud (asterisk). Moreover, the bilateral expression of *fli1a* (red) and *lef1* (blue) was absent homozygous *cloche* mutant embryos (G), compared to the wild type siblings (F, higher magnification f). (H,I) Confocal maximum intensity projections of fluorescent double *in situ* hybridization of *fli1a* (red) and *lef1* (green) (H, higher magnification h) and subsequent software based co-localization analysis (I, higher magnification i) indicated co-expression of *lef1* in a subset of *fli1a* expressing cells.

Fig. 4. EC specification is induced by Wnt3a and mediated via Lef1. (A,B) Morpholino (MO)-mediated knockdown of *wnt3a* reduced the EC number (A, n = 14) in *Tg(kdrl:GFP)*^{s843} embryos compared to control (ctr.) MO (A, n = 19). Knockdown of other Wnt ligands, expressed in the zebrafish posterior LPM, did not significantly change EC numbers compared to ctr. MO injected embryos (A): *wnt9a* (n = 13), *wnt9b* (n = 14), *wnt8* (n = 19) or *wnt3* (n = 7). (C) MO-mediated knockdown or transient CRISPR-Cas9-mediated knockdown of *wnt3a* significantly reduced the EC volume in *Tg(kdrl:GFP)*^{s843} embryos (ctr. MO: n = 5; *wnt3a* MO: n = 8; ctr. CRISPR: n = 5; *wnt3a* CRISPR: n = 8). Agarose gel electrophoresis of *wnt3a* CRISPR genotyping showed an undigested putatively mutated PCR product (*wnt3a* CRISPR fragment). Non-mutated wild type fragments were cut by PstI digest. (D,E) MO-mediated knockdown of *lef1* reduced the EC number (D, n = 10) compared to ctr. MO (D, n = 38) in *Tg(kdrl:GFP)*^{s843} embryos. Knockdown of any of the other Tcf-transcription factors did not significantly change EC numbers compared to ctr. MO injected embryos (D): *tcf7* (n = 30), *tcf7l1a* (n = 23), *tcf7l1b* (n = 28) or *tcf7l2* (n = 32). (F) Heatshock induced Wnt ligand overexpression using *Tg(hsp70l:wnt8-GFP)*^{w34} (indicated as *hs:wnt8*) increased the EC volume in *Tg(kdrl:mCherry)*^{s896} embryos (F, n = 7) compared to control siblings (F, n = 12). In contrast, heatshock induced overexpression of Wnt signaling inhibitor Dkk1 using *Tg(hsp70l:dkk1-GFP)*^{w32} (indicated as *hs:dkk1*) decreased the EC volume (F, n = 5) compared to control siblings. (G) EC and erythrocyte cell volume analysis in *lef1*^{u767} mutant embryos. Embryos carrying heterozygous and homozygous *lef1*^{u767} mutations showed reduced EC volumes (G, upper panel, wt sibling: n = 14; *lef1*$^{u767/+}$: n = 18; *lef1*$^{u767/u767}$: n = 10), but increased erythrocyte volumes (G, lower panel, wt sibling: n = 14; *lef1*$^{u767/+}$: n = 19; *lef1*$^{u767/u767}$: n = 9) compared to wild type siblings. (H) MO-mediated knockdown of *lef1* decreased the EC volume (H, upper panel, n = 6) compared to ctr. MO (H, upper panel, n = 7) in *Tg(kdrl:GFP)*^{s843} embryos, but increased the erythrocyte volume (H, lower panel, n = 7) compared to ctr. MO (H, lower panel, n = 7) in *Tg(gata1:GFP)*^{la781} embryos. Overactivation of Wnt signaling in *lef1*-deficient embryos using BIO restored EC volume and erythrocyte volume nearly to control levels (H, upper and lower panel, n = 7). All values represent mean ± SD. *p < 0.05, **p < 0.01, ***p < 0.001; Student's *t*-test.

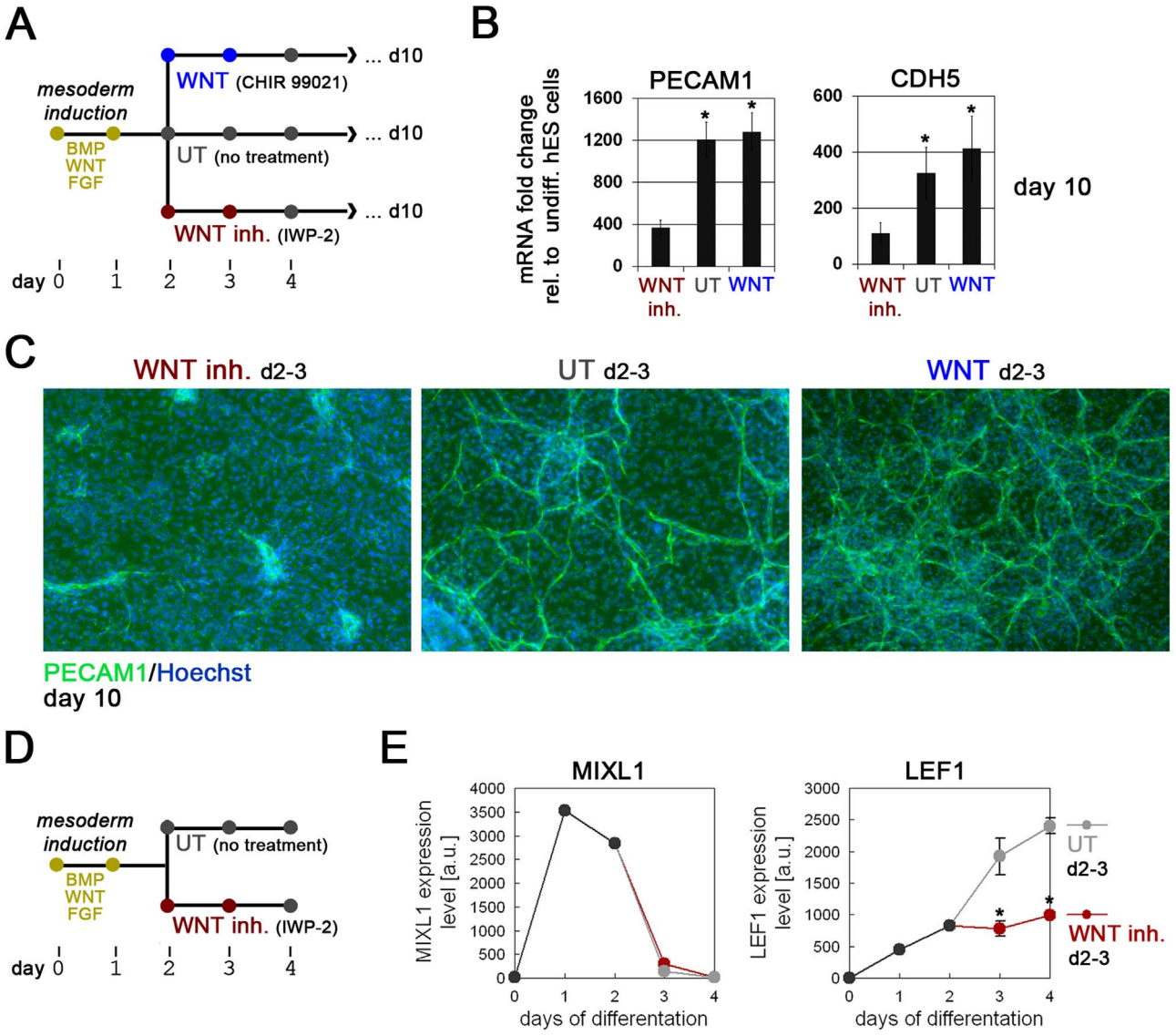

Fig. 6. Wnt signaling promotes EC differentiation in human ES cells. (A) Differentiation protocol for investigating the effects of Wnt inhibition after an initial treatment with BMP, Wnt, and FGF to induce a mesodermal progenitor state. (B) RT-qPCR analysis of endothelial markers PECAM1 and CDH5 on day 10 of differentiation, using distinct differentiation conditions illustrated in A. (C) Immunocytochemical analysis of PECAM1 expression on day 10 using distinct differentiation conditions illustrated in A. (D-F) Gene expression time-course analysis of the primitive streak marker MIXL1 (E) as well as LEF1 (F) (microarray data). Note the decrease in LEF1 expression by inhibition of autocrine WNT signaling on days 2 and 3.

vascular plexus (Palis and Yoder, 2001). However, our observations focused only on the first wave of EC specification, and therefore on putative arterial ECs. The later specification of venous angioblasts (Jin et al., 2007; Kohli et al., 2013) might be regulated differently.

We clearly show that Wnt signaling acts on the *fli1a*-positive and *kdrl*- and *gata1*-negative cell population. This is in agreement with previous reports, that Fli1a acts upstream of EC and blood development in zebrafish and frogs (Liu et al., 2008), but in contrast to the early onset of *etv2* expression potentially restricted to the EC lineage (Kohli et al., 2013). However, we believe that this early progenitor population is very fragile and easily disturbed by manipulations, for example heatshock induced overexpression of mCherry did affect the differentiation of ECs and often ended up targeted to the *gata1*-positive erythrocyte population (data not shown).

It has been suggested earlier, that Wnt signaling could be involved in the EC versus erythrocyte fate specification (Gore et al., 2011; Kazanskaya et al., 2008). But despite availability of global and conditional knockouts used for Wnt signaling manipulation, this role of Wnt signaling has not been uncovered in mice. The reasons for that might be, that Wnt signaling is required for mesoderm induction and that the experiments involve targeting of an early progenitor population. Hence, the murine global Wnt3 knockout is unable to form a primitive streak, mesoderm or node (Liu et al., 1999). In zebrafish due to a partial genome duplication two Wnt3 copies exist: Wnt3 and Wnt3a. These genes can function redundantly, e.g. during induction of the Shh-secreting middiencephalic organizer (Mattes et al., 2012), but might also have diverged in their spatiotemporal action. In line with the latter, only Wnt3a knockdown (but not Wnt3 knockdown) affected EC specification (Fig. 4). Conditional approaches in mice manipulating the Wnt signaling pathway, e.g. vascular specifically (Cattelino et al., 2003), only target specified ECs, and therefore fail to elucidate the role of Wnt signaling on the progenitor population. This is also in line with the temporally very restricted responsiveness of our novel transgenic Wnt reporter lines in the *fli1a*-positive progenitor population (Fig. 1), which indicates the fast speed of progenitor differentiation, making targeting of these cells more difficult. However, previous reports indicate, that Wnt3 positively regulates EC specification in mouse embryoid bodies (Wang et al., 2006) and pharmacological activation of

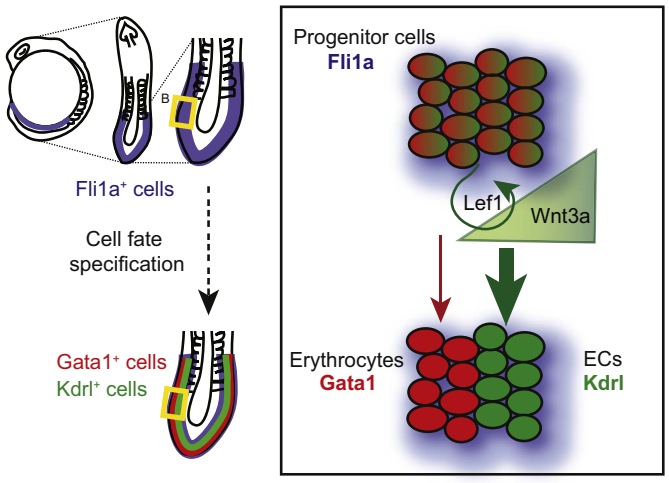

Fig. 7. Wnt3a-Lef1-signaling acts on *fli1a*-positive progenitor cells to induce EC specification. Progenitors of ECs and primitive erythrocytes derive from the posterior LPM and are Fli1a-positive (blue). Within the Fli1a-positive progenitor cell population, the medial expressed Wnt3a induces Lef1 expression, which leads to an upregulation of Lef1 expression as well as to endothelial cell fate specification (positive feedback loop). ECs are characterized by Kdrl expression (green) and erythrocytes by Gata1 expression (red). The future erythrocytes sort to a more lateral position and do not upregulate Lef1.

Wnt signaling induced EC differentiation from human pluripotent stem cells (Lian et al., 2014).

In recent years, there are a few reports demonstrating that later in development Wnt signaling is involved in subspecification of cell fates within the EC lineage (Grainger et al., 2016; Nicenboim et al., 2015; Ulrich et al., 2016; Vanhollebeke et al., 2015). During definitive hematopoiesis for example, Wnt9a-induced Wnt signaling is required in hemogenic endothelial (HE) cells (Chanda et al., 2013; Grainger et al., 2016), which differentiate from the specified EC population and are characterized by upregulated expression of hematopoietic marker genes (e.g. *runx1*) (Eliades et al., 2016; Fujimoto et al., 2001). Interestingly, *in vitro* studies using human pluripotent stem cells indicate, that definitive hematopoietic progenitors require Wnt signaling during specification, whereas primitive hematopoietic progenitors can be generated using Wnt signaling inhibitory conditions, which is in line with our findings ((Sturgeon et al., 2014), Fig. 3). Furthermore, the specification of lymphatic ECs from specialized angioblasts within the posterior cardinal vein is induced by Wnt5b signals (Nicenboim et al., 2015), whereas during brain development Wnt7a/7b signals promote tip cell selection and brain capillary sprouting via Gpr124-Reck (Daneman et al., 2009; Posokhova et al., 2015; Ulrich et al., 2016; Vanhollebeke et al., 2015). These findings together with our data argue for a specialized, temporally and spatially controlled function of Wnt ligands during embryonic development and for a role of Wnt signaling during EC fate specification in different developmental contexts.

In our study, we show for the first time that Wnt3a regulates the cell fate decision between ECs and primitive erythrocytes directly and only during the very short specification phase in the Fli1a-positive progenitor cell population (Fig. 7). We demonstrate, that Wnt signaling promotes EC specification via Lef1, while limiting erythrocyte specification at the same time. Our findings add to understanding of lineage specification during early embryonic development and provide insights into the balanced regulation of ECs and primitive erythrocytes.

Conflict of interest

The authors declare, that they have no conflict of interest.

Acknowledgements

We thank David Trevor and Friedemann Kiefer for critical comments and suggestions on the manuscript. We are grateful to Reinhild Bussmann for excellent fish husbandry and Stefan Volkery for imaging assistance.

This work was supported by the Deutsche Forschungsgemeinschaft (HE4585/2-1; HE4585/3-1) and the North Rhine-Westphalia "return fellowship" awarded to W. H., K.S.G. was initially funded by a CEDAD graduate school fellowship. B.G. and J.R. were supported by the Chemical Genomics Centre of the Max Planck Society. S.S. was supported by NIH R01HL107369.

Appendix A. Supplementary material

Supplementary data associated with this article can be found in the online version at doi:10.1016/j.ydbio.2017.08.004.

References

Angers, S., Moon, R.T., 2009. Proximal events in Wnt signal transduction. Nat. Rev. Mol. Cell Biol. 10, 468–477.
Aulehla, A., Wiegraebe, W., Baubet, V., Wahl, M.B., Deng, C., Taketo, M., Lewandoski, M., Pourquie, O., 2008. A beta-catenin gradient links the clock and wavefront systems in mouse embryo segmentation. Nat. Cell Biol. 10, 186–193.
Behrens, J., Jerchow, B.-A., Würtele, M., Grimm, J., Asbrand, C., Wirtz, R., Kühl, M., Wedlich, D., Birchmeier, W., 1998. Functional interaction of an axin homolog, conductin, with β-catenin, APC, and GSK3β. Science 280, 596–599.
Behrens, J., von Kries, J.P., Kuhl, M., Bruhn, L., Wedlich, D., Grosschedl, R., Birchmeier, W., 1996. Functional interaction of beta-catenin with the transcription factor LEF-1. Nature 382, 638–642.
Blaschke, K., Ebata, K.T., Karimi, M.M., Zepeda-Martinez, J.A., Goyal, P., Mahapatra, S., Tam, A., Laird, D.J., Hirst, M., Rao, A., Lorincz, M.C., Ramalho-Santos, M., 2013. Vitamin C induces Tet-dependent DNA demethylation and a blastocyst-like state in ES cells. Nature 500, 222–226.
Blum, Y., Belting, H.G., Ellertsdottir, E., Herwig, L., Luders, F., Affolter, M., 2008. Complex cell rearrangements during intersegmental vessel sprouting and vessel fusion in the zebrafish embryo. Dev. Biol. 316, 312–322.
Brown, L.A., Rodaway, A.R.F., Schilling, T.F., Jowett, T., Ingham, P.W., Patient, R.K., Sharrocks, A.D., 2000. Insights into early vasculogenesis revealed by expression of the ETS-domain transcription factor Fli-1 in wild-type and mutant zebrafish embryos. Mech. Dev. 90, 237–252.
Buckles, G.R., Thorpe, C.J., Ramel, M.C., Lekven, A.C., 2004. Combinatorial Wnt control of zebrafish midbrain-hindbrain boundary formation. Mech. Dev. 121, 437–447.
Bussmann, J., Schulte-Merker, S., 2011. Rapid BAC selection for tol2-mediated transgenesis in zebrafish. Development 138, 4327–4332.
Cattelino, A., Liebner, S., Gallini, R., Zanetti, A., Balconi, G., Corsi, A., Bianco, P., Wolburg, H., Moore, R., Oreda, B., Kemler, R., Dejana, E., 2003. The conditional inactivation of the beta-catenin gene in endothelial cells causes a defective vascular pattern and increased vascular fragility. J. Cell Biol. 162, 1111–1122.
Chanda, B., Ditadi, A., Iscove, N.N., Keller, G., 2013. Retinoic acid signaling is essential for embryonic hematopoietic stem cell development. Cell 155, 215–227.
Chen, B., Dodge, M.E., Tang, W., Lu, J., Ma, Z., Fan, C.W., Wei, S., Hao, W., Kilgore, J., Williams, N.S., Roth, M.G., Amatruda, J.F., Chen, C., Lum, L., 2009. Small molecule-mediated disruption of Wnt-dependent signaling in tissue regeneration and cancer. Nat. Chem. Biol. 5, 100–107.
Chi, N.C., Shaw, R.M., De Val, S., Kang, G., Jan, L.Y., Black, B.L., Stainier, D.Y., 2008. Foxn4 directly regulates tbx2b expression and atrioventricular canal formation. Genes Dev. 22, 734–739.
Choi, K., Kennedy, M., Kazarov, A., Papadimitriou, J.C., Keller, G., 1998. A common precursor for hematopoietic and endothelial cells. Development 125, 725–732.
Clevers, H., Nusse, R., 2012. Wnt/beta-catenin signaling and disease. Cell 149, 1192–1205.
Covassin, L.D., Siekmann, A.F., Kacergis, M.C., Laver, E., Moore, J.C., Villefranc, J.A., Weinstein, B.M., Lawson, N.D., 2009. A genetic screen for vascular mutants in zebrafish reveals dynamic roles for Vegf/Plcg1 signaling during artery development. Dev. Biol. 329, 212–226.
Daneman, R., Agalliub, D., Zhoub, L., Kuhnertc, F., Kuoc, C.J., Barres, B.A., 2009. Wnt/-catenin signaling is required for CNS, but not non-CNS, angiogenesis. Proc. Natl. Acad. Sci. USA 106, (6422-6422).
Dorsky, R.I., Sheldahl, L.C., Moon, R.T., 2002. A transgenic Lef1/beta-catenin-dependent reporter is expressed in spatially restricted domains throughout zebrafish development. Dev. Biol. 241, 229–237.
Eliades, A., Wareing, S., Marinopoulou, E., Fadlullah, M.Z., Patel, R., Grabarek, J.B., Plusa, B., Lacaud, G., Kouskoff, V., 2016. The hemogenic competence of endothelial progenitors is restricted by runx1 silencing during embryonic development. Cell Rep. 15, 2185–2199.
Franco, C.A., Liebner, S., Gerhardt, H., 2009. Vascular morphogenesis: a Wnt for every vessel? Curr. Opin. Genet. Dev. 19, 476–483.
Frank, S., Zhang, M., Scholer, H.R., Greber, B., 2012. Small molecule-assisted, line-independent maintenance of human pluripotent stem cells in defined conditions. PLoS One 7, e41958.
Fujimoto, T., Ogawa, M., Minegishi, N., Yoshida, H., Yokomizo, T., Yamamoto, M.,

Nishikawa, S., 2001. Step-wise divergence of primitive and definitive haematopoietic and endothelial cell lineages during embryonic stem cell differentiation. Genes Cells 6, 1113–1127.
Gering, M., Rodaway, A.R., Gottgens, B., Patient, R.K., Green, A.R., 1998. The SCL gene specifies haemangioblast development from early mesoderm. EMBO J. 17, 4029–4045.
Gore, A.V., Swift, M.R., Cha, Y.R., Lo, B., McKinney, M.C., Li, W., Castranova, D., Davis, A., Mukouyama, Y.S., Weinstein, B.M., 2011. Rspo1/Wnt signaling promotes angiogenesis via Vegfc/Vegfr3. Development 138, 4875–4886.
Grainger, S., Richter, J., Palazon, R.E., Pouget, C., Lonquich, B., Wirth, S., Grassme, K.S., Herzog, W., Swift, M.R., Weinstein, B.M., Traver, D., Willert, K., 2016. Wnt9a is required for the aortic amplification of nascent hematopoietic stem cells. Cell Rep. 17, 1595–1606.
Greber, B., Coulon, P., Zhang, M., Moritz, S., Frank, S., Muller-Molina, A.J., Arauzo-Bravo, M.J., Han, D.W., Pape, H.C., Scholer, H.R., 2011. FGF signalling inhibits neural induction in human embryonic stem cells. EMBO J. 30, 4874–4884.
Habib, S.J., Chen, B.C., Tsai, F.C., Anastassiadis, K., Meyer, T., Betzig, E., Nusse, R., 2013. A localized Wnt signal orients asymmetric stem cell division in vitro. Science 339, 1445–1448.
Haferkamp, I., Schmitz-Esser, S., Linka, N., Urbany, C., Collingro, A., Wagner, M., Horn, M., Neuhaus, H.E., 2004. A candidate NAD+ transporter in an intracellular bacterial symbiont related to Chlamydiae. Nature 432, 622–625.
Hamm, M.J., Kirchmaier, B.C., Herzog, W., 2016. Sema3d controls collective endothelial cell migration by distinct mechanisms via Nrp1 and PlxnD1. J. Cell Biol. 215, 415–430.
Helker, C.S., Schuermann, A., Karpanen, T., Zeuschner, D., Belting, H.G., Affolter, M., Schulte-Merker, S., Herzog, W., 2013. The zebrafish common cardinal veins develop by a novel mechanism: lumen ensheathment. Development 140, 2776–2786.
Helker, C.S., Schuermann, A., Pollmann, C., Chng, S.C., Kiefer, F., Reversade, B., Herzog, W., 2015. The hormonal peptide Elabela guides angioblasts to the midline during vasculogenesis. Elife 4.
Herzog, W., Zeng, X., Lele, Z., Sonntag, C., Ting, J.-W., Chang, C.-Y., Hammerschmidt, M., 2003. Adenohypophysis formation in the zebrafish and its dependence on sonic hedgehog. Dev. Biol. 254, 36–49.
Hesselson, D., Anderson, R.M., Beinat, M., Stainier, D.Y., 2009. Distinct populations of quiescent and proliferative pancreatic beta-cells identified by HOTcre mediated labeling. Proc. Natl. Acad. Sci. USA 106, 14896–14901.
Jagannathan-Bogdan, M., Zon, L.I., 2013. Hematopoiesis. Development 140, 2463–2467.
Jao, L.E., Wente, S.R., Chen, W., 2013. Efficient multiplex biallelic zebrafish genome editing using a CRISPR nuclease system. Proc. Natl. Acad. Sci. USA 110, 13904–13909.
Jin, S.W., Beis, D., Mitchell, T., Chen, J.N., Stainier, D.Y., 2005. Cellular and molecular analyses of vascular tube and lumen formation in zebrafish. Development 132, 5199–5209.
Jin, S.W., Herzog, W., Santoro, M.M., Mitchell, T.S., Frantsve, J., Jungblut, B., Beis, D., Scott, I.C., D'Amico, L.A., Ober, E.A., Verkade, H., Field, H.A., Chi, N.C., Wehman, A.M., Baier, H., Stainier, D.Y., 2007. A transgene-assisted genetic screen identifies essential regulators of vascular development in vertebrate embryos. Dev. Biol. 307, 29–42.
Kazanskaya, O., Ohkawara, B., Heroult, M., Wu, W., Maltry, N., Augustin, H.G., Niehrs, C., 2008. The Wnt signaling regulator R-spondin 3 promotes angioblast and vascular development. Development 135, 3655–3664.
Kohli, V., Schumacher, J.A., Desai, S.P., Rehn, K., Sumanas, S., 2013. Arterial and venous progenitors of the major axial vessels originate at distinct locations. Dev. Cell 25, 196–206.
Lawson, N.D., Weinstein, B.M., 2002. In vivo imaging of embryonic vascular development using transgenic zebrafish. Dev. Biol. 248, 307–318.
Lee, C.Y., Vogeli, K.M., Kim, S.H., Chong, S.W., Jiang, Y.J., Stainier, D.Y., Jin, S.W., 2009. Notch signaling functions as a cell-fate switch between the endothelial and hematopoietic lineages. Curr. Biol. 19, 1616–1622.
Lee, D., Park, C., Lee, H., Lugus, J.J., Kim, S.H., Arentson, E., Chung, Y.S., Gomez, G., Kyba, M., Lin, S., Janknecht, R., Lim, D.S., Choi, K., 2008. ER71 acts downstream of BMP, Notch, and Wnt signaling in blood and vessel progenitor specification. Cell Stem Cell 2, 497–507.
Lekven, A.C., Thorpe, C.J., Waxman, J.S., Moon, R.T., 2001. Zebrafish wnt8 encodes two wnt8 proteins on a bicistronic transcript and is required for mesoderm and neurectoderm patterning. Dev. Cell 1, 103–114.
Leung, J.Y., Kolligs, F.T., Wu, R., Zhai, Y., Kuick, R., Hanash, S., Cho, K.R., Fearon, E.R., 2002. Activation of AXIN2 expression by beta-catenin-T cell factor. A feedback repressor pathway regulating Wnt signaling. J. Biol. Chem. 277, 21657–21665.
Lian, X., Bao, X., Al-Ahmad, A., Liu, J., Wu, Y., Dong, W., Dunn, K.K., Shusta, E.V., Palecek, S.P., 2014. Efficient differentiation of human pluripotent stem cells to endothelial progenitors via small-molecule activation of WNT signaling. Stem Cell Rep. 3, 804–816.
Liu, F., Walmsley, M., Rodaway, A., Patient, R., 2008. Fli1 acts at the top of the transcriptional network driving blood and endothelial development. Curr. Biol. 18, 1234–1240.
Liu, P.T., Wakamiya, M., Shea, M.J., Albrecht, U., Behringer, R.R., Bradley, A., 1999. Requirement for Wnt3 in vertebrate axis formation. Nat. Genet. 22, 361–365.
Loh, K.M., van Amerongen, R., Nusse, R., 2016. Generating cellular diversity and spatial form: wnt signaling and the evolution of multicellular animals. Dev. Cell 38, 643–655.
Long, Q.M., Meng, A.M., Wang, H., Jessen, J.R., Farrell, M.J., Lin, S., 1997. GATA-1 expression pattern can be recapitulated in living transgenic zebrafish using GFP reporter gene. Development 124, 4105–4111.
Maretto, S., Cordenonsi, M., Dupont, S., Braghetta, P., Broccoli, V., Hassan, A.B., Volpin, D., Bressan, G.M., Piccolo, S., 2003. Mapping Wnt/beta-catenin signaling during mouse development and in colorectal tumors. Proc. Natl. Acad. Sci. USA 100, 3299–3304.
Martin, B.L., Kimelman, D., 2012. Canonical Wnt signaling dynamically controls multiple stem cell fate decisions during vertebrate body formation. Dev. Cell 22, 223–232.
Mattes, B., Weber, S., Peres, J., Chen, Q., Davidson, G., Houart, C., Scholpp, S., 2012. Wnt3 and Wnt3a are required for induction of the mid-diencephalic organizer in the caudal forebrain. Neural Dev. 7.
Meijer, L., Skaltsounis, A.L., Magiatis, P., Polychronopoulos, P., Knockaert, M., Leost, M., Ryan, X.P., Vonica, C.A., Brivanlou, A., Dajani, R., Crovace, C., Tarricone, C., Musacchio, A., Roe, S.M., Pearl, L., Greengard, P., 2003. GSK-3-selective inhibitors derived from Tyrian purple indirubins. Chem. Biol. 10, 1255–1266.
Moro, E., Ozhan-Kizil, G., Mongera, A., Beis, D., Wierzbicki, C., Young, R.M., Bournele, D., Domenichini, A., Valdivia, L.E., Lum, L., Chen, C., Amatruda, J.F., Tiso, N., Weidinger, G., Argenton, F., 2012. In vivo Wnt signaling tracing through a transgenic biosensor fish reveals novel activity domains. Dev. Biol. 366, 327–340.
Nasevicius, A., Larson, J., Ekker, S.C., 2000. Distinct requirements for zebrafish angiogenesis revealed by a VEGF-A morphant. Yeast 17, 294–301.
Nicenboim, J., Malkinson, G., Lupo, T., Asaf, L., Sela, Y., Mayseless, O., Gibbs-Bar, L., Senderovich, N., Hashimshony, T., Shin, M., Jerafi-Vider, A., Avraham-Davidi, I., Krupalnik, V., Hofi, R., Almog, G., Astin, J.W., Golani, O., Ben-Dor, S., Crosier, P.S., Herzog, W., Lawson, N.D., Hanna, J.H., Yanai, I., Yaniv, K., 2015. Lymphatic vessels arise from specialized angioblasts within a venous niche. Nature 522, 56–61.
Ouspenskaia, T., Matos, I., Mertz, A.F., Fiore, V.F., Fuchs, E., 2016. WNT-SHH antagonism specifies and expands stem cells prior to niche formation. Cell 164, 156–169.
Palis, J., Yoder, M.C., 2001. Yolk-sac hematopoiesis: the first blood cells of mouse and man. Exp. Hematol. 29, 927–936.
Posokhova, E., Shukla, A., Seaman, S., Volate, S., Hilton, M.B., Wu, B., Morris, H., Swing, D.A., Zhou, M., Zudaire, E., Rubin, J.S., St Croix, B., 2015. GPR124 functions as a WNT7-specific coactivator of canonical beta-catenin signaling. Cell Rep. 10, 123–130.
Proulx, K., Lu, A., Sumanas, S., 2010. Cranial vasculature in zebrafish forms by angioblast cluster-derived angiogenesis. Dev. Biol. 348, 34–46.
Reis, M., Liebner, S., 2013. Wnt signaling in the vasculature. Exp. Cell Res. 319, 1317–1323.
Reischauer, S., Stone, O.A., Villasenor, A., Chi, N., Jin, S.W., Martin, M., Lee, M.T., Fukuda, N., Marass, M., Witty, A., Fiddes, I., Kuo, T., Chung, W.S., Salek, S., Lerrigo, R., Alsio, J., Luo, S., Tworus, D., Augustine, S.M., Mucenieks, S., Nystedt, B., Giraldez, A.J., Schroth, G.P., Andersson, O., Stainier, D.Y., 2016. Cloche is a bHLH-PAS transcription factor that drives haemato-vascular specification. Nature 535, 294–298.
Risau, W., Flamme, I., 1995. Vasculogenesis. Annu. Rev. Cell Dev. Biol. 11, 73–91.
Schoenebeck, J.J., Keegan, B.R., Yelon, D., 2007. Vessel and blood specification override cardiac potential in anterior mesoderm. Dev. Cell 13, 254–267.
Shalaby, F., Rossant, J., Yamaguchi, T.P., Gertsenstein, M., Wu, X.F., Breitman, M.L., Schuh, A.C., 1995. Failure of blood-island formation and vasculogenesis in Flk-1-deficient mice. Nature 376, 62–66.
Shimizu, N., Kawakami, K., Ishitani, T., 2012. Visualization and exploration of Tcf/Lef function using a highly responsive Wnt/beta-catenin signaling-reporter transgenic zebrafish. Dev. Biol. 370, 71–85.
Stainier, D.Y., Weinstein, B.M., Detrich, H.W., 3rd, Zon, L.I., Fishman, M.C., 1995. Cloche, an early acting zebrafish gene, is required by both the endothelial and hematopoietic lineages. Development 121, 3141–3150.
Stoick-Cooper, C.L., Weidinger, G., Riehle, K.J., Hubbert, C., Major, M.B., Fausto, N., Moon, R.T., 2007. Distinct Wnt signaling pathways have opposing roles in appendage regeneration. Development 134, 479–489.
Sturgeon, C.M., Ditadi, A., Awong, G., Kennedy, M., Keller, G., 2014. Wnt signaling controls the specification of definitive and primitive hematopoiesis from human pluripotent stem cells. Nat. Biotechnol. 32, 554–561.
Sumanas, S., Lin, S., 2006. Ets1-related protein is a key regulator of vasculogenesis in zebrafish. PLoS Biol. 4, e10.
Thisse, C., Thisse, B., 2008. High-resolution in situ hybridization to whole-mount zebrafish embryos. Nat. Protoc. 3, 59–69.
Thompson, M.A., Ransom, D.G., Pratt, S.J., MacLennan, H., Kieran, M.W., Detrich, H.W., 3rd, Vail, B., Huber, T.L., Paw, B., Brownlie, A.J., Oates, A.C., Fritz, A., Gates, M.A., Amores, A., Bahary, N., Talbot, W.S., Her, H., Beier, D.R., Postlethwait, J.H., Zon, L.I., 1998. The cloche and spadetail genes differentially affect hematopoiesis and vasculogenesis. Dev. Biol. 197, 248–269.
Traver, D., Paw, B.H., Poss, K.D., Penberthy, W.T., Lin, S., Zon, L.I., 2003. Transplantation and in vivo imaging of multilineage engraftment in zebrafish bloodless mutants. Nat. Immunol. 4, 1238–1246.
Ulrich, F., Carretero-Ortega, J., Menendez, J., Narvaez, C., Sun, B., Lancaster, E., Pershad, V., Trzaska, S., Veliz, E., Kamei, M., Prendergast, A., Kidd, K.R., Shaw, K.M., Castranova, D.A., Pham, V.N., Lo, B.D., Martin, B.L., Raible, D.W., Weinstein, B.M., Torres-Vazquez, J., 2016. Reck enables cerebrovascular development by promoting canonical Wnt signaling. Development 143, 147–159.
Valdivia, L.E., Young, R.M., Hawkins, T.A., Stickney, H.L., Cavodeassi, F., Schwarz, Q., Pullin, L.M., Villegas, R., Moro, E., Argenton, F., Allende, M.L., Wilson, S.W., 2011. Lef1-dependent Wnt/beta-catenin signalling drives the proliferative engine that maintains tissue homeostasis during lateral line development. Development 138, 3931–3941.
Vanhollebeke, B., Stone, O.A., Bostaille, N., Cho, C., Zhou, Y., Maquet, E., Gauquier, A., Cabochette, P., Fukuhara, S., Mochizuki, N., Nathans, J., Stainier, D.Y., 2015. Tip

cell-specific requirement for an atypical Gpr124- and Reck-dependent Wnt/beta-catenin pathway during brain angiogenesis. Elife 4.
Villefranc, J.A., Amigo, J., Lawson, N.D., 2007. Gateway compatible vectors for analysis of gene function in the zebrafish. Dev. Dyn. 236, 3077–3087.
Vogeli, K.M., Jin, S.W., Martin, G.R., Stainier, D.Y., 2006. A common progenitor for haematopoietic and endothelial lineages in the zebrafish gastrula. Nature 443, 337–339.
Wang, H., Charles, P.C., Wu, Y., Ren, R., Pi, X., Moser, M., Barshishat-Kupper, M., Rubin, J.S., Perou, C., Bautch, V., Patterson, C., 2006. Gene expression profile signatures indicate a role for Wnt signaling in endothelial commitment from embryonic stem cells. Circ. Res. 98, 1331–1339.
Weidinger, G., Thorpe, C.J., Wuennenberg-Stapleton, K., Ngai, J., Moon, R.T., 2005. The Sp1-related transcription factors sp5 and sp5-like act downstream of Wnt/beta-catenin signaling in mesoderm and neuroectoderm patterning. Curr. Biol. 15, 489–500.
Westerfield, M., 1993. The Zebrafish Book. University of Oregon Press, Eugene, OR.